ChemPubSoc Europe

DOI: 10.1002/chem.201902381

CHEMISTRY A European Journal Full Paper

Gold Catalysis

Gold-Catalyzed Regiospecific Annulation of Unsymmetrically Substituted 1,5-Diynes for the Precise Synthesis of Bispentalenes

Sara Tavakkolifard+,[a] Kohei Sekine+,[a] Lisa Reichert,[a] Mina Ebrahimi,[a] Ketevan Museridz,[a] Elena Michel,[a] Frank Rominger,[a] Rasool Babaahmadi,[b] Alireza Ariafard,*[b] Brian F. Yates,*[b] Matthias Rudolph,[a] and A. Stephen K. Hashmi*[a, c]

Abstract: Precise control of the selectivity in organic synthesis is important to access the desired molecules. We demonstrate a regiospecific annulation of unsymmetrically substituted 1,2-di(arylethynyl)benzene derivatives for a geometry-controlled synthesis of linear bispentalenes, which is one of the promising structures for material science. A gold-catalyzed annulation of unsymmetrically substituted 1,2-di(arylethynyl)benzene could produce two isomeric pentalenes, but both electronic and steric effects on the aromatics at the terminal position of the alkyne prove to be crucial for the selectivity; especially a regiospecific annulation was achieved with sterically blocked substituents; namely, 2,4,6-trimetyl benzene or 2,4-dimethyl benzene. This approach enables the geometrically controlled synthesis of linear bispentalenes from 1,2,4,5-tetraethynylbenzene or 2,3,6,7-tetraethynylnaphthalene. Moreover, the annulation of a series of tetraynes with a different substitution pattern regioselectively provided the bispentalene scaffolds. A computational study revealed that this is the result of a kinetic control induced by the bulky NHC ligands.

Introduction

Antiaromatic molecules have received much attention due to unique optoelectronic properties. Pentalene as well as the structurally similar indenofluorene[1] is one of the important core structures for material science. Due to the low stability of the pure pentalene core,[2] various syntheses of dibenzo[*a*,*e*]-pentalenes, which are stabilized by the fused aromatic moieties, have been developed.[3] The properties of pentalene are of high interest for organic semiconductors. Especially, π-extended pentalenes prove to act as p- or n-type organic transistors, although tuning optoelectronic properties by the introduction of functional groups are still desirable for higher performance.[4] Therefore, the development of modular synthetic methods to access polycyclic π-extended pentalenes is a promising research topic.

Homogeneous gold catalysis has received much attention, and due to the mild carbophilic π Lewis acidity of the gold catalyst, the field majorly contributed to the intensive development of nucleophilic addition reactions to unsaturated carbon–carbon multiple bonds.[5] For instance, the gold-catalyzed annulation of diyne compounds enabled the synthesis of extended π-conjugated compounds, such as azahelicene, polycyclic indole and benzothiophen derivatives.[6] Our recent work also contributed to the gold-catalyzed synthesis of dibenzo[*a*,*e*]pentalene and quinoxaline/phenazine-fused pentalene derivatives from 1,5-diynes.[3n,t] Moreover, the gold catalyst led to both U-shaped and S-shaped bispentalenes from the readily available tetra(arylethynyl)benzenes and -naphthalenes, albeit fortunately those mixtures could be separated (Scheme 1, top).[4e] During that study, the naphthalene-based linear bispentalene (S-shaped) was found to be a highly suitable scaffold for transistor applications. In these symmetric tetraynes, however, the chemoselectivity towards U-shaped and S-shaped bispentalenes is not controlled. Unsymmetrically substituted diynes or tetraynes as substrates could be a method to selectively synthesize specific isomers, still it is unknown whether the selectivity will be pronounced enough to deliver only one

[a] S. Tavakkolifard,+ Dr. K. Sekine,+ L. Reichert, M. Ebrahimi, K. Museridz, E. Michel, Dr. F. Rominger, Dr. M. Rudolph, Prof. Dr. A. S. K. Hashmi
Organisch-Chemisches Institut
Heidelberg University
Im Neuenheimer Feld 270
69120 Heidelberg (Germany)
E-mail: hashmi@hashmi.de

[b] R. Babaahmadi, Prof. A. Ariafard, Prof. B. F. Yates
School of Physical Sciences (Chemistry)
University of Tasmania
Private Bag 75
Hobart TAS 7001 (Australia)
E-mail: alirezaa@utas.edu.au
Brian.Yates@utas.edu.au

[c] Prof. Dr. A. S. K. Hashmi
Chemistry Department, Faculty of Science
King Abdulaziz University
Jeddah 21589 (Saudi Arabia)

[+] These authors contributed equally to this work.

Supporting information and the ORCID identification number(s) for the author(s) of this article can be found under: https://doi.org/10.1002/chem.201902381.

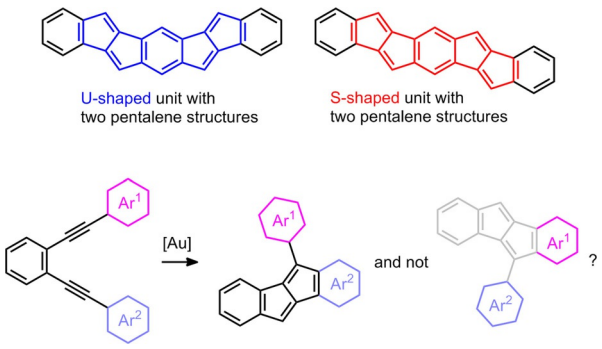

Scheme 1. Possible selectivity control by different aryl groups in the gold-catalyzed annulation of unsymmetrically substituted 1,5-diynes.

isomer (Scheme 1, bottom). From the synthetic point of view, it would be interesting to see if the reaction of unsymmetrically substituted 1,5-diynes can be controlled by electronic or steric effects, which would allow to control the precise regiochemistry and thus the geometry in the synthesis of pentalene derivatives. Herein, we report a study of selectivity control in the gold-catalyzed annulation of unsymmetrically substituted 1,5-diynes, and the use of these principles in the regiospecific synthesis of S-shaped benzene- and naphthalene-based bispentalenes by an "inside-out" bidirectional approach. In addition, we investigated an "outside-in" mode of cyclization, tetraynes with different substitution patterns successfully provided bispentalenes, which with respect to the overall synthetic route represents a much more convergent and thus flexible approach. The opto-electronic properties of the obtained bispentalene derivatives are also reported.

Results and Discussion

During the annulation of a symmetric 1,5-diyne, one alkyne acts as a nucleophile and the other alkyne as the electrophile. If electron-rich and electron-deficient alkynes are arranged in an unsymmetrical substrate, the annulation could proceed regiospecifically. We first prepared the unsymmetrically substituted diynes **1** with methoxy (**1a**), fluoro (**1b**), and trifluoromethyl substituents (**1c**), and attempted the gold-catalyzed reactions with them (Table 1). The annulation of methoxy-substituted

Table 1. Electronic effect on the selectivity.

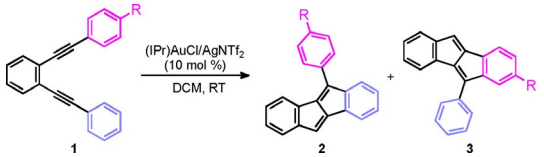

Entry[a]	R		Time [h]	Yield [%][b]	2:3[c]
1	OMe	**1a**	1	40	96:4
2	F	**1b**	1	62	42:58
3	CF_3	**1c**	16	29	6:94

[a] **1** (0.05 mmol), catalysts (0.005 mmol) in solvent (1 mL). [b] Combined yield of **2** and **3**. [c] Determined by ^{1}H NMR of the crude mixture.

diyne gave a mixture of isomers **2a** and **3a** in 40% yield with a ratio of 96:4 (entry 1). Fluoro-substituted diyne **1b** afforded isomers **2b** and **3b** in 62% yield in a ratio of 42:58 (entry 2). When a trifluoromethyl group (**1c**), which is a strong electron-withdrawing group, was attached to the aromatic ring, the ratio of **2c** and **3c** was 6:94 (entry 3). Overall, the results demonstrated that the selectivity can be controlled by the electronic properties with the electron-rich alkyne acting as nucleophile, while the electron-deficient alkyne serves as the electrophile, even though the yield lower and the isomers are inseparable.

To explore another mode of substituent control of the selectivity, two *o*-positions of the aryl group on the alkyne were blocked by methyl groups, which probably inhibits the approach of the gold catalysts to the sterically more hindered alkyne, even though a cyclization of the vinyl cation and mesitylene followed by a 1,2-methyl shift might still be possible. The gold catalysts promoted the reaction of the diyne **1d** and afforded the desired pentalene **2d** in 94% yield (Table 2,

Table 2. Reaction of mesitylene-substituted diynes.

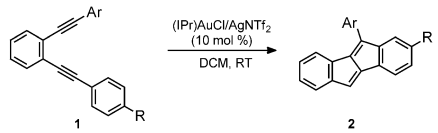

Entry[a]	Ar	R		Time [h]	Yield [%][b]
1	mesityl	H	**1d**	1	94
2	mesityl	OMe	**1e**	3	63
3[c]	mesityl	CF_3	**1f**	20	41
4	mesityl	Br	**1g**	20	60
5	2,4-dimethylbenzene	H	**1h**	1	91

[a] **1** (0.05 mmol), catalysts (0.005 mmol) in solvent (2 mL). [b] Isolated yield. [c] 40 °C.

entry 1). Methoxy- or trifluoromethyl-substituted diynes **1e** and **1f** were also converted to pentalenes **2e** and **2f** in 63 and 41% yield, respectively (entries 2 and 3). The annulation of bromo-substituted diyne **1g** gave pentalene **2g** in 60% yield, which could be useful for further transformations by common coupling reactions (entry 4). The mesityl group indeed enables a control of the pentalene synthesis. It is interesting to note that the reaction of the 2,4-dimethylbenzene-substituted diyne **1h** resulted in the clean formation of the corresponding pentalene **2h** in 91% yield and no generation of the pentalene **3h** (entry 5). As shown in Scheme 2, the gold-catalyzed reaction of diyne **1h** possibly leads to two intermediates **Ia** and **Ib**. Vinyl cation intermediate **Ib** might be unfavorable because the cyclization of **Ib**, which should proceed through a planar configuration is probably prohibited by the steric hindrance between the gold catalyst and the *o*-methyl substituent of the aromatic moiety. This results in the selective formation of **2h**. This step could be crucial for controlling the reaction of the mesitylene-substituted diyne **1d**. Overall, those results indicated that regiospecific annulation was achieved by the introduction of a mesityl group or 2,4-dimethylbenzene.

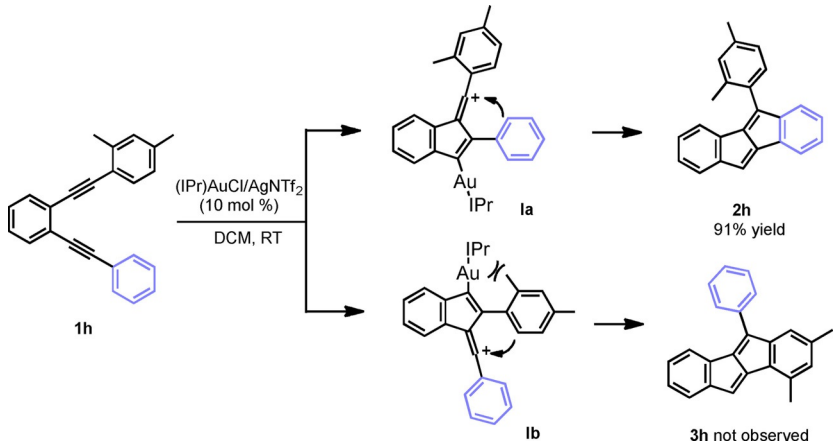

Scheme 2. Gold-catalyzed reaction to form pentalene **2h**.

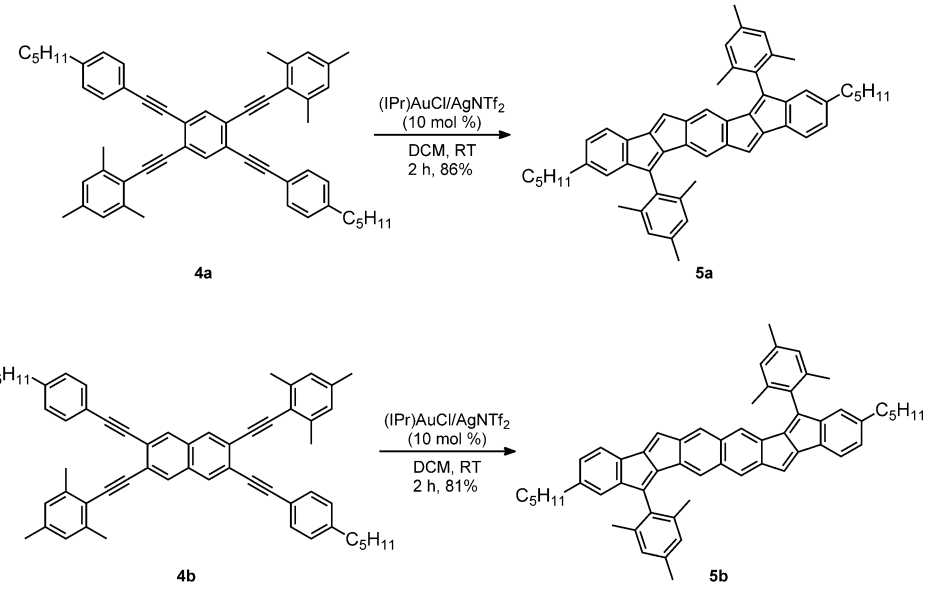

Scheme 3. Top) Gold-catalyzed annulation of 1,2,4,5-tetra(ethynyl)benzene (**4a**), and bottom) 2,3,6,7-tetra(ethynyl)naphthalene (**4b**) .

Based on the results with the diynes being blocked at the *o*-positions, the selective synthesis of S-shape bispentalenes should be feasible. We then designed and synthesized the benzene- and naphthalene-based tetraynes **4a** and **4b** with mesitylene (Scheme 3). The tetraynes **4a** and **4b** were conveniently prepared by sequential Sonogashira-coupling reactions of 1,4-dibromo-2,5-diiodobenzene or 3,7-dibromonaphthalene-2,6-diyl-bis(trifluoromethanesulfonate). Using (IPr)AuCl/$AgNTf_2$, the benzene-based tetrayne **4a** was completely consumed within 2 h, the corresponding linear bispentalene **5a** was obtained in 81% yield as a reddish-brown solid. In addition, the annulation of naphthalene-based tetrayne **4b** with (IPr)AuCl/$AgNTf_2$ proceeded at room temperature and gave the linear bispentalene **5b** in 86% yield as a red solid.

The connectivity of **5b** in the solid state was confirmed by X-ray crystallography (Figure 1). Due to the mesityl group, the

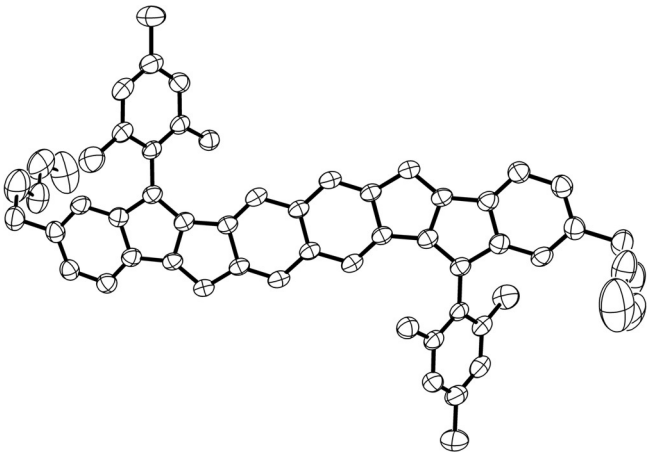

Figure 1. Solid-state molecular structure of **5b**.

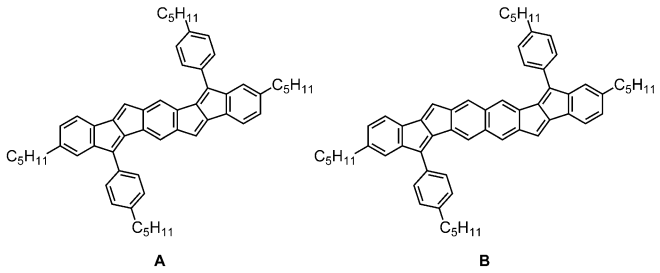

Figure 2. Previously reported bispentalenes **A** and **B**.

previously reported *n*-pentyl substituted S-shape bispentalene **B** (Figure 2)[4e] shows significantly smaller torsion angles (34.2–37.9°) between the pentalene core and the peripheral aryl group than pentalene **5b** (63.5–69.3°).

We considered tetrayne **6a**, having a different substitution pattern, as another approach to access the bispentalene scaffold. It could potentially afford two isomers, **7a** and **8a**, because the second annulation could occur on both carbon atoms of the intermediate **IIa** (Scheme 4). Indeed, the intramolecular annulation with 5 mol% of gold catalysts in dichloroethane afforded pentalenes **7a** and **8a** in 20 and 72% yield, respectively. The structure of **8a** was unambiguously confirmed by single-crystal X-ray crystallography (Figure 3). Interestingly, the pentalene core and the peripheral mesityl group are nearly vertical and the two mesityl groups are parallel.

When the cyclization of **6a** was performed using (IPr)AuCl/$AgNTf_2$, isomers **7a** and **8a** were produced in a 22:78 ratio. In our previous report,[4e] the bulkiness of the ligand had a significant effect on the ratio of the resulting bispentalene isomers. Therefore, a set of differently sized ligands on the catalysts was investigated to prove this effect on the selectivity of isomeric bispentalenes **7a** and **8a.** Pre-activated [(IPr)Au(NCMe)]SbF_6 and [(IPr)Au]NTf_2 catalysts[7] gave the same results as (IPr)AuCl/$AgNTf_2$ (Table 3, entries 2 and 6). On the other hand, the PPh_3 ligand only gave poor yields of the products **7a** and **8a** (entry 3). No reaction took place with a nitrogen acyclic carbene (NAC) complex (entry 4). As expected, no reaction occurred in the complete absence of a gold catalyst, using only

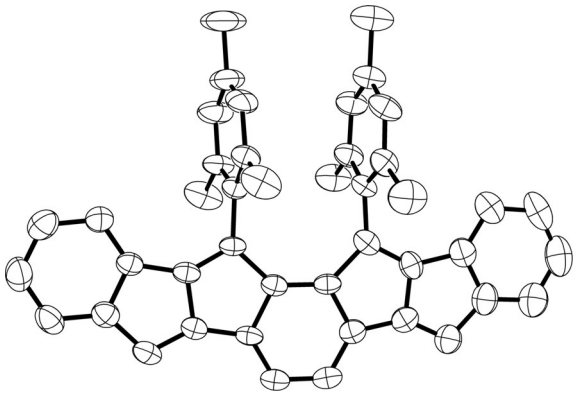

Figure 3. Solid-state molecular structure of **8a**.

Table 3. Examination of different ligands on the gold catalysts with substrate **6a**.

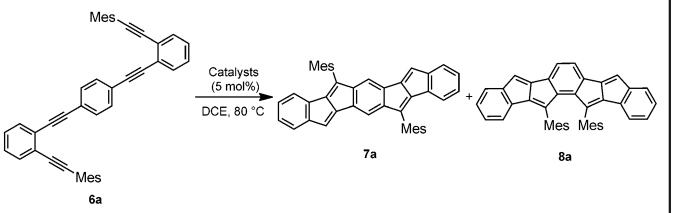

Entry[a]	Catalyst	Time [h]	Yield [%][b] **7a**:**8a**	Ratio **7a**:**8a**
1	(IPr)AuCl/$AgNTf_2$	2	20:72	22:78
2	[(IPr)Au(NCMe)]SbF_6	1.5	21:72	23:77
3	$Ph_3PAuNTf_2$	3	15:55	21:79
4	NACAuCl/$AgSbF_6$	4	ND	ND
5	(IPr)*AuCl/$AgNTf_2$	3.5	62[c]	4:96[d]
6	[(IPr)Au]NTf_2	2.5	18:71	20:80
7	$AgNTf_2$	4.5	ND	ND

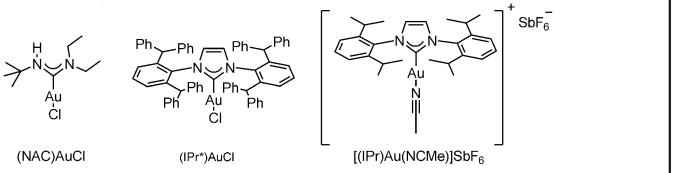

[a] Reaction performed in a vial in DCE (1 mL), **6a** (0.02 mmol) and catalyst (0.005 mmol). [b] Isolated yield. [c] Combined yield of **7a** and **8a**. [d] Determined by ^1H NMR.

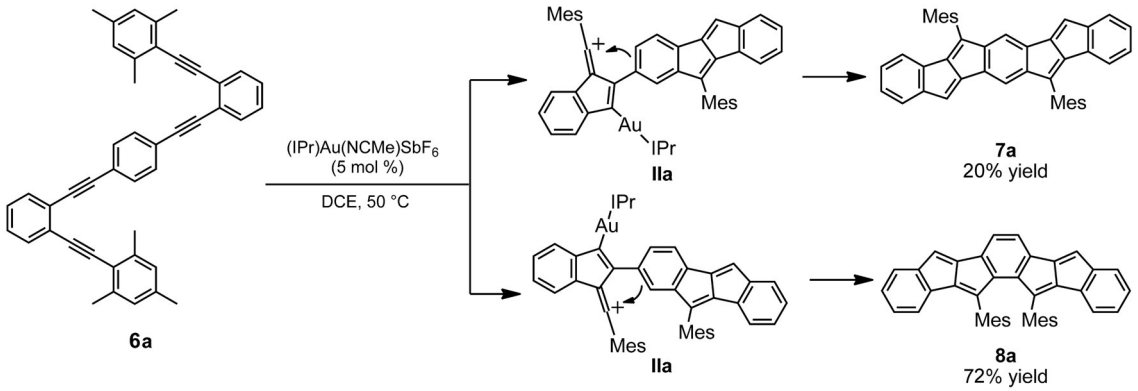

Scheme 4. Gold-catalyzed reaction to form bispentalenes **7a** and **8a**.

$AgNTf_2$ (entry 7). The short ligand screening finally revealed that the sterically bulky IPr* ligand[8] increases the ratio of pentalen **8a** (entry 5). This can be rationalized by the steric hindrance between the mesitylene substituent and the gold complex on the intermediate **IIa**, which ultimately leads to the formation of product **8a**.

The selective formation of **8a** was investigated by using M06-2X-CPCM/BS2//B3LYP-CPCM/BS1 calculations. It was found that the selectivity is mainly controlled by a steric repulsion between the mesityl substituent and the IPr ligand in **TS-1b** (Figure 4). This destabilizing interaction is absent in **TS-1a**, causing this transition structure to be 0.3 kcal mol^{-1} lower in energy than in **TS-1b**. To support this assertion, the IPr carbene ligand was replaced by the IMe carbene ligand, in which the bulky N-substituents of IPr are replaced by methyl groups. The results starting from this new model system are shown in Figure 5. In contrast to the real system in which **TS-1a** is calculated to be slightly lower in energy than **TS-1b**, for the less bulky model system, the energy order of the transition structures becomes reversed. In this case, **TS-1b-M** is calculated to be 2.0 kcal mol^{-1} lower in energy than **TS-1a-M** (Figure 5). The energy order of transition structures **TS-1b-M** and **TS-1a-M** is most likely set by the thermodynamic aspects of the transformation. Indeed, **7a** is about 6 kcal mol^{-1} more stable than **8a**, resulting in **TS-1b-M** lying lower in energy than **TS-1a-M**. Thus, although the formation of **7a** is thermodynamically favored over **8a**, the steric interaction between the IPr ligand and the Mes substituent in **TS1-b** leads to less **7a** than **8a** being formed.

Figure 4 shows quite similar energy values of **TS-1a** and **TS-1b** with **TS-1a** being lower in energy by 0.3 kcal mol^{-1}. This is consistent with the experimental 22:78 ratio of the two products. Figure 5 shows a higher difference in energy for **TS-1a-M** and **TS-1b-M** with a reversed order, now with **TS-1b-M** being lower. Since the repulsive interactions of the two aryl substituents in **TS-1a** and **TS-1a-M** are almost identical, this clearly indicates that the ligand–aryl steric interaction in **TS-1b** is stronger than that in **TS-1b-M**.

Next, several electron-withdrawing and electron-donating substituents on the aromatic moieties were investigated using $[(IPr)Au(NCMe)]SbF_6$ as the catalyst. In the case of tetrayne **6a**, the gold-catalyzed reaction afforded bispentalenes **7a** and **8a** in a ratio of 22:78 (Table 4, entry 1). Fluoro-substituted substrate **6b** led to the separable bispentalene isomers **7b** and **8b** with a ratio of 35:65 in 25 and 55% yield, respectively (entry 2). Tetrayne **6c** with dimethyl substituents on the outer aromatic moieties exhibit higher selectivity towards the formation of **8c** over **7c** (entry 3, 91:9 ratio, 36 and 3% yield, respectively), although the overall yield significantly dropped. These results indicate that the substituents on outer aromatics influence the selectivity of the transformation.

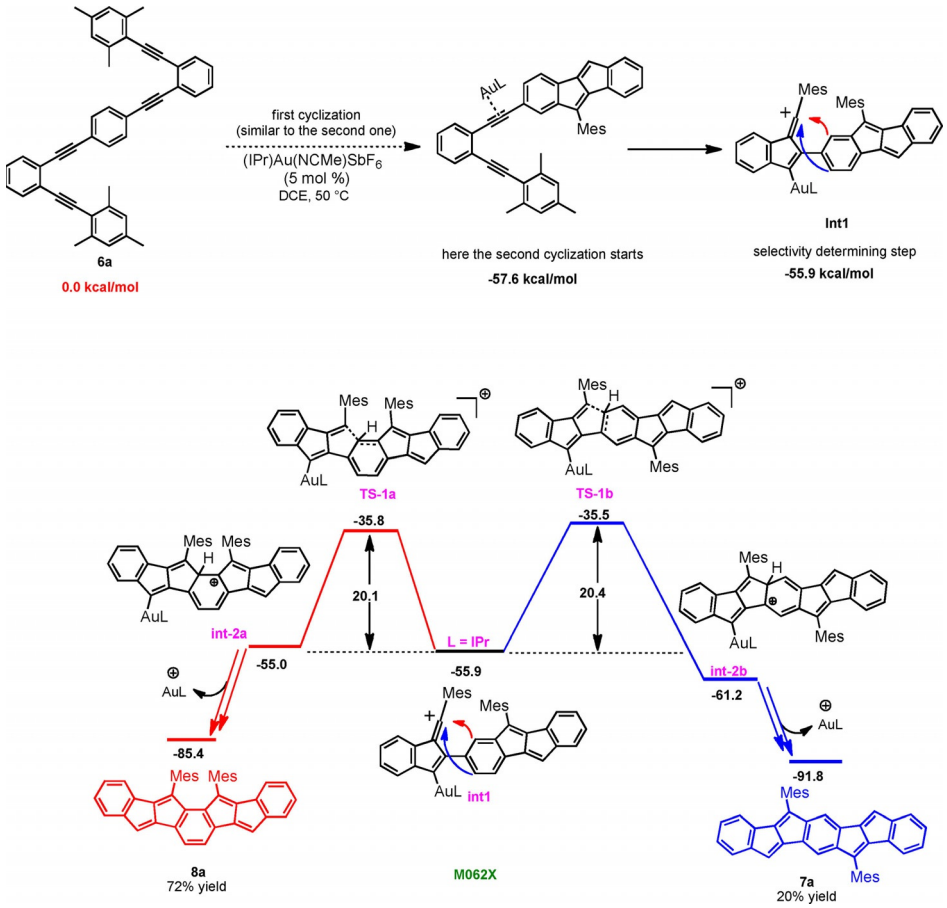

Figure 4. The selectivity-determining step with the IPr carbene ligand (energies in kcal mol^{-1}).

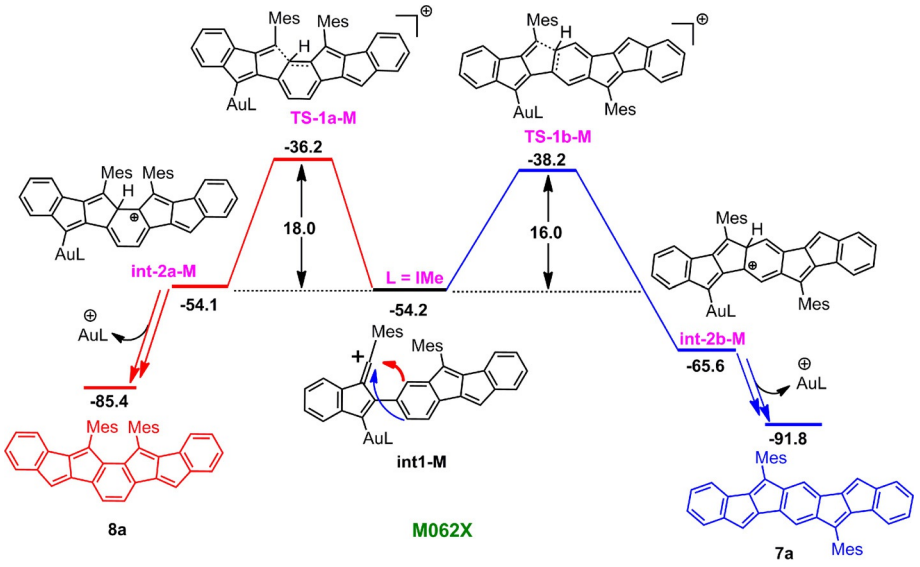

Figure 5. The selectivity-determining step with the smaller IMe carbene ligand (energies in kcal mol^{-1}).

Table 4. Bispentalene derivatives.[a]

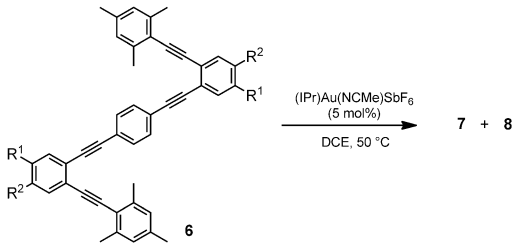

Entry	Compound	R^1	R^2	Time [h]	Yield [%][b] 7:8
1	**6a**	H	H	**2**	20:72
2	**6b**	F	H	**2**	25:55
3	**6c**	Me	Me	**3**	3:36

[a] Reaction performed in a vial in DCE (1 mL), **6** (0.05 mmol) and catalyst (0.005 mmol). [b] Yield of isolated product.

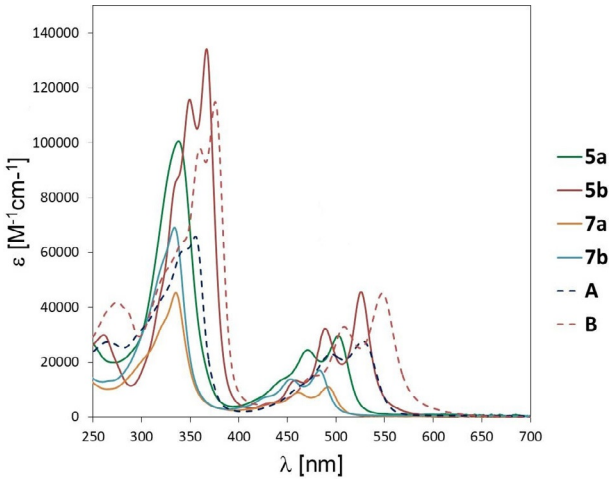

Figure 6. UV–Vis absorption of **5a**, **5b**, **7a**, and **7b**.

The optical properties of bispentalenes **5a**, **5b**, **7a** and **7b** were examined by UV–Vis absorption spectroscopy in dichloromethane (Figure 6). Based on previous work,[4e] the two characteristic absorptions (λ = 450–550 nm) of **5a**, **7a**, and **7b** might be assigned to HOMO→LUMO+1 and HOMO−1→LUMO transitions. The introduction of mesityl groups has a significant effect on the absorption. Thus, the absorption peaks (λ_{max} = 474 and 502 nm) of mesitylene-substituted **5a** were red-shifted (30 nm) compared to the S-shaped benzene-based bispentalene **A** (λ_{max} = 496 and 532 nm). A similar tendency was observed between naphthalene-based bispentalenes **5b** (λ_{max} = 490 and 525 nm) and **B** (λ_{max} = 510 and 550 nm). In addition, from the comparison of **5a** (λ_{max} = 474 and 502 nm) and **7a** (λ_{max} = 460 and 490 nm), differences on the substitution position of mesityl groups caused significant blue-shift.

The HOMO and LUMO levels of the series of bispentalenes **5a**, **5b**, **7a**, and **7b** in CH_2Cl_2 were estimated by cyclic voltammetry (Table 5). Compared to the previously synthesized benzene-based bispentalene **A** and naphthalene-based bispentalene **B** (Figure 2), the HOMO levels of **5a** (−5.24 eV) and **5b** (−5.50 eV) are lower than the HOMO levels of the corresponding compounds **A** (−5.20 eV) and **B** (−5.38 eV). The LUMO levels of **5a** (−3.11 eV) and **5b** (−2.93 eV) are significantly higher than the LUMO level of the corresponding compounds **A** (−3.23 eV) and **B** (−3.09 eV), which resulted in the larger HOMO–LUMO energy gap of **5a** and **5b**. Based on the solid-state structure of **5b** (Figure 1), the peripheral mesitylene might contribute less to the core π-system, which could have an effect on the HOMO and LUMO energy levels. The HOMO and LUMO levels of the S-shaped bispentalenes **7a** (HOMO = −5.30 eV, LUMO = −3.18 eV) and **7b** (HOMO = −5.40 eV, LUMO = −3.25 eV) are lower compared to **5a**. The HOMO–LUMO gaps for **7a** and **7b** (E_{gap} = 2.15 eV) are not significantly different from that of **5a** (E_{gap} = 2.13 eV).

Table 5. Cyclic voltammetry data and estimated HOMO and LUMO energies.

	E_{ox1} [V]	E_{red1} [V]	E_{HOMO}[c] [eV]	E_{LUMO}[c] [eV]	E_{gap} [eV]
A[a]	0.40	−1.57	−5.20	−3.23	1.98
5a[a]	0.44	−1.69	−5.24	−3.11	2.13
B[a]	0.58	−1.71	−5.38	−3.09	2.29
5b[a]	0.70	−1.87	−5.50	−2.93	2.57
7a[b]	0.51	−1.65	−5.30	−3.15	2.15
7b[b]	0.60	−1.55	−5.40	−3.25	2.15

[a] Cyclic voltammetry in CH_2Cl_2 containing 0.1 M nBu_4NPF_6 with ferrocene on a Pt working electrode, a Pt/Ti counter electrode, and a Ag reference electrode at a scan rate of 0.2 V s^{-1}. All potentials are given versus the Fc^+/Fc couple used as an internal standard. [b] Electrochemical data obtained at a scan rate of 0.2 V s^{-1} in CH_2Cl_2 containing 0.1 M nBu_4NPF_6 on a glassy carbon working electrode, a Pt/Ti counter electrode, and Ag reference electrode. [c] HOMO and LUMO energy levels in eV were approximated using the equation HOMO = −(4.80+E_{ox}), LUMO = −(4.80+E_{red}), E_{gap} = LUMO−HOMO.

Conclusions

We report the regiospecific annulation of unsymmetrically substituted 1,2-di(arylethynyl)benzene derivatives. Both electronic and steric effects on the aromatic moieties of the substrates are crucial for the selectivity. Especially, the introduction of sterically blocked substituents, such as 2,4,6-trimetylbenzene or 2,4-dimethylbenzene, enabled the regiospecific annulation. This method provided the geometrically-controlled synthesis of S-shaped bispentalenes from 1,2,4,5-tetraethynlbenzene or 2,3,6,7-tetraethynlnaphthalene. Moreover, the annulation of a series of tetraynes with a different substitution pattern regioselectively provided bispentalenes. Our computational studies showed that **7a** is the thermodynamic product of the reaction, whereas **8a** is the kinetic product, preferentially formed with bulky NHC ligands (like IPr, but better IPr*).

Acknowledgements

S.T is grateful for a Ph.D. scholarship from the Hans-Böckler-Stiftung.

Conflict of interest

The authors declare no conflict of interest.

Keywords: gold · homogeneous catalysis · pentalenes · polycyclic aromatic hydrocarbons · regiospecific

[1] C. K. Frederickson, B. D. Rose, M. M. Haley, *Acc. Chem. Res.* **2017**, *50*, 977.
[2] T. Bally, S. Chai, M. Neuenschwander, Z. Zhu, *J. Am. Chem. Soc.* **1997**, *119*, 1869.
[3] Review for the synthesis and optoelectronic properties of pentalenes, please see a) M. Saito, *Symmetry* **2010**, *2*, 950. For recent publications about monobenzopentalene, see b) P. Rivera-Fuentes, M. V. W. Rekowski, W. B. Schweizer, J.-P. Gisselbrecht, C. Boudon, F. Diederich, *Org. Lett.* **2012**, *14*, 4066; c) G. London, M. V. W. Rekowski, O. Dumele, W. B. Schweizer, J.-P. Gisselbrecht, C. Boudon, F. Diederich, *Chem. Sci.* **2014**, *5*, 965; d) S. Kato, S. Kuwako, N. Takahashi, T. Kijima, Y. Nakamura, *J. Org. Chem.* **2016**, *81*, 7700. For dibenzopentalene, see e) K. Katsumoto, C. Kitamura, T. Kawase, *Eur. J. Org. Chem.* **2011**, 4885; f) M. Saito, Y. Hashimoto, T. Tajima, K. Ishimura, S. Nagase, M. Minoura, *Chem. Asian J.* **2012**, *7*, 480; g) A. S. K. Hashmi, M. Wieteck, I. Braun, P. Nosel, L. Jongbloed, M. Rudolph, F. Rominger, *Adv. Synth. Catal.* **2012**, *354*, 555; h) C. Chen, M. Harhausen, R. Liedtke, K. Bussmann, A. Fukazawa, S. Yamaguchi, J. L. Petersen, C. G. Daniliuc, R. Frçhlich, G. Kehr, G. Erker, *Angew. Chem. Int. Ed.* **2013**, *52*, 5992; *Angew. Chem.* **2013**, *125*, 6108; i) T. Maekawa, Y. Segawa, K. Itami, *Chem. Sci.* **2013**, *4*, 2369; j) J. Zhao, K. Oniwa, N. Asao, Y. Yamamoto, T. Jin, *J. Am. Chem. Soc.* **2013**, *135*, 10222; k) J. Shen, D. Yuan, Y. Qiao, X. Shen, Z. Zhang, Y. Zhong, Y. Yi, X. Zhu, *Org. Lett.* **2014**, *16*, 4924; l) C. Chen, M. Harhausen, A. Fukazawa, S. Yamaguchi, R. Frçhlich, C. G. Daniliuc, J. L. Petersen, G. Kehr, G. Erker, *Chem. Asian J.* **2014**, *9*, 1671; m) B. Wei, H. Li, W.-X. Zhang, Z. Xi, *Organometallics* **2016**, *35*, 1458; n) T. Wurm, J. Bucher, S. B. Duckworth, M. Rudolph, F. Rominger, A. S. K. Hashmi, *Angew. Chem. Int. Ed.* **2017**, *56*, 3364; *Angew. Chem.* **2017**, *129*, 3413; o) K. Takahashi, S. Ito, R. Shintani, K. Nozaki, *Chem. Sci.* **2017**, *8*, 101; p) H. Oshima, A. Fukazawa, S. Yamaguchi, *Angew. Chem. Int. Ed.* **2017**, *56*, 3270; *Angew. Chem.* **2017**, *129*, 3318; q) A. Konishi, Y. Okada, M. Nakano, K. Sugisaki, K. Sato, T. Takui, M. Yasuda, *J. Am. Chem. Soc.* **2017**, *139*, 15284; r) D. C. Grenz, M. Schmidt, D. Kratzert, B. Esser, *J. Org. Chem.* **2018**, *83*, 656; s) T. Wurm, E. C. Rediger, J. Schulmeister, S. Koser, M. Rudolph, F. Rominger, U. H. F. Bunz, A. S. K. Hashmi, *Chem. Eur. J.* **2018**, *24*, 2735; t) K. Sekine, F. Stuck, J. Schulmeister, T. Wurm, D. Zetschok, F. Rominger, M. Rudolph, A. S. K. Hashmi, *Chem. Eur. J.* **2018**, *24*, 12515.
[4] p-type: a) T. Kawase, T. Fujiwara, C. Kitamura, A. Konishi, Y. Hirano, K. Matsumoto, H. Kurata, T. Kubo, S. Shinamura, H. Mori, E. Miyazaki, K. Takimiya, *Angew. Chem. Int. Ed.* **2010**, *49*, 7728; *Angew. Chem.* **2010**, *122*, 7894; b) C. Liu, X. Xu, W. Zhu, X. Zhu, W. Hu, Z. Li, Z. Wang, *Chem. Eur. J.* **2015**, *21*, 17016; c) G. Dai, J. Chang, W. Zhang, S. Bai, K.-W. Huang, J. Xu, C. Chi, *Chem. Commun.* **2015**, *51*, 503; d) C. Li, C. Liu, Y. Li, X. Zhu, A. Wang, *Chem. Commun.* **2015**, *51*, 693; e) K. Sekine, J. Schulmeister, F. Paulus, K. P. Goetz, F. Rominger, M. Rudolph, J. Zaumseil, A. S. K. Hashmi, *Chem. Eur. J.* **2019**, *25*, 216; n-type: f) M. Nakano, I. Osaka, K. Takimiya, T. Koganezawa, *J. Mater. Chem. C* **2014**, *2*, 64; g) M. Nakano, I. Osaka, K. Takimiya, *J. Mater. Chem. C* **2015**, *3*, 283; h) G. Dai, J. Chang, L. Jing, C. Chi, *J. Mater. Chem. C* **2016**, *4*, 8758; i) A. S. K. Hashmi, R. Salathé, W. Frey, *Chem. Eur. J.* **2006**, *12*, 6991.
[5] a) D. Pflästerer, A. S. K. Hashmi, *Chem. Soc. Rev.* **2016**, *45*, 1331; b) R. Dorel, A. M. Echavarren, *Chem. Rev.* **2015**, *115*, 9028; c) L. Zhang, *Acc. Chem. Res.* **2014**, *47*, 877; d) L. P. Liu, G. B. Hammond, *Chem. Soc. Rev.* **2012**, *41*, 3129; e) H. Ohno, *Isr. J. Chem.* **2013**, *53*, 869; f) A. Fürstner, *Chem. Soc. Rev.* **2009**, *38*, 3208; g) N. Bongers, N. Krause, *Angew. Chem. Int. Ed.* **2008**, *47*, 2178; *Angew. Chem.* **2008**, *120*, 2208; h) A. Fürstner, P. W. Davies, *Angew. Chem. Int. Ed.* **2007**, *46*, 3410; *Angew. Chem.* **2007**, *119*, 3478; i) A. S. K. Hashmi, G. J. Hutchings, *Angew. Chem. Int. Ed.* **2006**, *45*, 7896; *Angew. Chem.* **2006**, *118*, 8064; j) A. S. K. Hashmi, *Chem. Rev.* **2007**, *107*, 3180; k) D. J. Gorin, F. D. Toste, *Nature* **2007**, *446*, 395; l) for early results, see: A. S. K. Hashmi, L. Schwarz, J.-H. Choi, T. M. Frost, *Angew. Chem. Int. Ed.* **2000**, *39*, 2285; *Angew. Chem.* **2000**, *112*, 2382; m) A. S. K. Hashmi, T. M. Frost, J. W. Bats, *J. Am. Chem. Soc.* **2000**, *122*, 11553.
[6] a) A. M. Asiri, A. S. K. Hashmi, *Chem. Soc. Rev.* **2016**, *45*, 4471; b) A. S. K. Hashmi, *Acc. Chem. Res.* **2014**, *47*, 864; c) I. Braun, A. M. Asiri, A. S. K. Hashmi, *ACS Catal.* **2013**, *3*, 1902.
[7] a) P. de Frémont, N. Marion, S. P. Nolan, *J. Organomet. Chem.* **2009**, *694*, 551; for alternative routes to unsaturated NHC-gold(I) complexes, see: b) D. Riedel, T. Wurm, K. Graf, M. Rudolph, F. Rominger, A. S. K. Hashmi, *Adv. Synth. Catal.* **2015**, *357*, 1515.
[8] A. Collado, A. Gómez-Suárez, A. R. Martin, A. M. Z. Slawin, S. P. Nolan, *Chem. Commun.* **2013**, *49*, 5541.

Manuscript received: May 24, 2019
Revised manuscript received: July 6, 2019
Accepted manuscript online: July 16, 2019
Version of record online: August 28, 2019

